Technical note: Low meteorological influence found in 2019 Amazonia fires

Douglas I. Kelley[1]*, Chantelle Burton[2], Chris Huntingford[1], Megan A. J. Brown[1,3], Rhys Whitley[4], Ning Dong[5]

5 [1] UK Centre for Ecology & Hydrology, Wallingford, Oxfordshire, OX10 8BB, U.K.
[2] Met Office Hadley Centre, Fitzroy Road, Exeter. EX1 3PB
[3] School of Physical Sciences, The Open University, Walton Hall, Milton Keynes, MK7 6AA, UK
[4] Natural Perils Pricing, Commercial and Consumer Portfolio and Product, Suncorp Group, Sydney, Australia
[5] Department of Biological Sciences, Macquarie University, North Ryde, NSW 2109, Australia

10 *Correspondence to*: Douglas I. Kelley (douglas.i.kelley@gmail.com)

Abstract The sudden increase in Amazon fires early in the 2019 fire season made global headlines. While it has been heavily speculated that the fires were caused by deliberate human ignitions or human-induced landscape changes, there have also been suggestions that meteorological conditions could have played a role. Here, we ask two questions: were the 2019 fires in the Amazon unprecedented in the historical record?; and did the

15 meteorological conditions contribute to the increased burning? To answer this, we take advantage of a recently developed modelling framework which optimizes a simple burnt area model, and whose outputs are described as probability densities. This allowed us to test the probability of the 2019 fire season occurring due to meteorological conditions alone. We show that the burnt area was indeed higher than previous years in regions where there is already substantial deforestation activity in the Amazon, with 11% of the area recording the

20 highest early season (June-August) burnt area since the start of our observational record. However, areas outside of the regions of widespread deforestation show less burnt area than the historical average, and the optimized model shows that there is a 71% probability that this low burned area would have been expected over the entire Amazon region, including regions already witnessing deforestation and of high fire occurrence in 2019. We show that there is a <7% chance of the observed June-August fires being caused by meteorological conditions

25 alone, decreasing to <1% in Paraguay and Bolivia dry-forests and at the eastern end of the Amazons arc of deforestation. This suggests that changes in land use and land cover or land management are the likely drivers of the large increase in the 2019 early fire season burnt area. Burnt area for the peak of the fire season in September returned to levels expected from meteorology conditions in the arc of deforestation, potentially coinciding with a shift in policy from South American governments, but remained high in Bolivia and Paraguay.

30

1 Introduction

South American fires made global headlines in August 2019, with the largest increase in fire activity seen in nearly ten years (INPE, 2019; Lizundia-Loiola et al., 2020). Of the roughly 100,000 fires burning by the end of the month, around half were in the Amazon rainforest region (Andrade, 2019; INPE, 2019). While fires in drier savannah regions of South America such as the Cerrado are more common, fires in the rainforest are not a natural occurrence and are rarely ignited without human intervention (Aldersley et al., 2011). As such, fires in humid, tropical regions where the vegetation is not adapted to frequent burning (Kelley, 2014; Zeppel et al., 2015), have much higher tree mortality rates (Brando et al., 2014; Cochrane and Schulze, 1999; Pellegrini et al., 2017). As a result, an estimated 906,000 hectares of the Amazon biome was lost to fires in 2019 (Butler, 2017). The amount of carbon and trace gas emission was also a major concern given the high biomass of the areas being burnt, and smoke from these fires reached cities as far as São Paulo more than 2,700km away (Lovejoy and Nobre, 2019). Usually, small-scale fires in Amazonia are associated with deliberate but localised deforestation, although in dry years there is more risk of these fires escaping into much larger areas (Aragão et al., 2018). Hence the substantial increase in fires in 2019 sparked much debate about whether the level of burning was unprecedented, whether increased burning was driven by a drier than normal fire season and if raised levels of direct deforestation played a role (Arruda et al., 2019; Escobar, 2019).

The Amazon was not the only place with recent unusual and high fire activity, with large-scale fire events worldwide in the last couple of years including in the Arctic, Mediterranean, Australia, UK and the US. In November 2018 over 80 people were killed in the Camp fire in Paradise California, the most destructive in California's history, with the Camp, Woolsey and Carr Fires together costing an estimated $27 billion in damages (Nauslar et al., 2019). Hundreds of fires burnt throughout the 2019 summer in Siberia and Alaska, releasing over 150 Mega tonnes of CO_2 to the atmosphere. Also released were large quantities of black carbon with the potential to further accelerate local arctic ice melt (Patel, 2019). The UK saw some burning, including a peatland fire in north-east Sutherland that doubled Scotland's carbon emission for six days in May 2019 (Wiltshire et al., 2019). Between September 2019 and February 2020, fires across eastern Australian temperate woodlands burnt around 18.6 million hectares, destroyed over 5,900 buildings, and killed at least 34 people (Boer et al., 2020; RFS, 2019; Sanderson and Fisher, 2020). Unusual fire events such as these are expected to increase in frequency in the future from both changes in climate and socio-economic pressures on the landscape (Fonseca et al., 2019; Jones et al., 2020). Given the concerns raised and the extent to which much of these fire events captured the attention of the public and press in recent months, in the aftermath it is important to look at these events objectively. In particular, it is essential to determine if they were unusual in the context of the historical record and if so what might be new and emerging drivers.

There are many ways to assess drivers of historical fire events. Some studies simply correlate individual drivers with burnt area in isolation (Andela et al., 2017; Van Der Werf et al., 2008). However, these do not consider the complex interaction of multiple drivers on fire and are therefore unable to go beyond a loose attribution of a particular forcing to fire. Fire Danger Indices (FDIs), which can capture simultaneous drivers, are useful for

calculating the level of risk of a fire spreading and becoming severe in a particular area (de Groot et al., 2015). FDIs have been adapted to assess recent and future trends in climate on fire weather (Burton et al., 2018; Jolly et al., 2015) and attribute increases in fire risk to anthropogenic changes in climate (van Oldenborgh et al., 2020).

70 These metrics thereby provide rapid policy-relevant information for fire management (De Groot et al., 2010; Perry et al., 2020). However, FDIs do not account for available fuel or ignition, which differentiates them from fire observations such as burnt area, and makes them an unsuitable tool for assessing fire in the holistic context of weather, fuel dynamics, ignition and human land and fire management (Kelley and Harrison, 2014). Fire-enabled Land Surface Models (LSMs) can, however, account for these drivers (Kelley and Harrison, 2014;

75 Lasslop et al., 2016; Prentice et al., 2011b) to simulate a physical, observable measure of fire regimes, such as burnt area or number of fires (Rabin et al., 2017). However, most LSMs have been developed to study long-term, often decadal timescale carbon dynamics and therefore often fail to reproduce year-to-year patterns of fire with the required accuracy to be used to determine causes of individual fire seasons (Andela et al., 2017; Hantson et al., 2016, 2020). This lack of annual predictive capability has led to calls for simulation frameworks

80 that fuse statistical representations of fire drivers with modelling techniques, and that consider such interactions (Fisher and Koven, 2020; Krawchuk and Moritz, 2014; Sanderson and Fisher, 2020; Tollefson, 2018; Williams and Abatzoglou, 2016).

Kelley et al. (2019) recently developed a methodology which addresses this gap by coupling process representation found in simple fire enabled LSMs (Rabin et al., 2017) with a Bayesian inference framework.

85 This system can assess the contribution of different fire drivers directly from observations and track uncertainty in the model. We apply this methodology here, using monthly meteorological conditions and burnt area (BA) observations to constrain and drive the model, thus capturing interannual variability within the context of a changing meteorological conditions. We use this framework to answer the specific question: Did the meteorological conditions contribute to the Amazonia Fires of 2019?

90 **2 Methods**

We largely followed the modelling protocol and optimization framework from Kelley et al. (2019), which contains a more detailed description. Monthly burnt area (BA) is modelled as a product of limitations imposed by four controls: 1) fuel availability; 2) moisture in live and dead fuel; 3) anthropogenic and natural ignition; 4) both active suppression and landscape fragmentation effects from human land use (Table S1 in Supplement).

95 Each control is calculated as a linear combination of its respective drivers. The impact each control has on fire is represented by a logistic curve describing the maximum allowed burnt area. Overall burnt area is then the product of these four limitations.

We made a small number of changes to the previous modelling protocol in order to utilise near-real-time meteorological and fire variables so that we can produce relevant results that closely follow the fire event. We

100 used MODIS Collection 6 MCD64A1 burned area product (Giglio et al., 2018) as our target dataset and replaced actual over potential evapotranspiration in the moisture control with soil moisture (Table S1). We also used both the top 10cm and 10-200cm soil moisture (Kalnay et al., 1996) as independent moisture drivers in

order to capture the impact of previous drought years on deepwater availability for live fuel. As near-real-time

wetday information is also not available, we replaced wet days in the calculation of dead fuel drying potential

105 (Kelley et al., 2014) with a proxy for wetdays, using GPCP precipitation (Adler et al., 2003) (pr) based on

(Prentice et al., 2011a):

$$WD = 1 - e^{-wd \, x \, pr} \tag{1}$$

where wd is an optimized parameter.

All variables were resampled and, where necessary, interpolated to a monthly timestep as per Kelley et al.

110 (2019) although here too a resolution of 2.5°, which was the coarsest and most common grid across all variables

used. MCD64A1, soil moisture and equilibrium fuel moisture content were translated to a 2.5-degree grid as per

Kelley et al. (2014), using the "rgdal" (Bivand et al., 2016) and "raster" (Hijmans and van Etten, 2014) packages

in R (R Core Team, 2015). For MODIS Vegetation Continuous Fields (VCF) fractional covers (Dimiceli et al.,

2015), tiles were merged and resampled to the model grid using the "gdal" package (GDAL/OGR contributors,

115 2018). Land use, population density, precipitation, humidity, temperature and lightning, were processed using

the iris package (Met Office, 2013) with python version 3 (Python Software Foundation,

https://www.python.org/).

The model was optimised against MCD64A1 burned area (Giglio et al., 2018) for the period July 2002 to June

2018, which was the common years among all datasets (Table S2) over South America, south of 13°N. We used

120 the same Bayesian Inference technique as per Kelley et al (2019). For the purposes of this study, Bayes' theorem

states that the likelihood of the values of the set, ß, which contain our 23 unknown parameters (i.e. the 21

parameters from Kelley et al (2019), wd from equation 2, an error term parameter σ) and our known model

inputs, given a set of observations Y_s is proportional to the prior probability distribution of ß ($P(ß)$) multiplied

by the probability of Y_s given ß:

125 $$P(\beta|Y_s) \propto P(\beta) \cdot P(Y_s|\beta) \tag{2}$$

where $P(Y_s|ß)$ was defined as a truncated normal distribution:

$$P(Y_s|ß) = \aleph(F, \sigma) = \frac{N}{\sigma\sqrt{2\pi}} exp \left\{ \Sigma_i^N \left(\frac{y_i - BA_i}{\sigma} \right)^2 \right\} \tag{3}$$

and where i represents an individual data point, y_i is the burnt area observations and N is the observation

sample size.

130

The posterior solution was inferred for the models' parameters ($P(Y_s|ß)$) using a Metropolis-Hastings Markov

Chain Monte Carlo (MCMC) step with the pymc3 python package (Salvatier et al., 2016), running 10 chains

each over 10,000 iterations. Unlike Kelley et al. (2019), we used all of the 44750 data points on our 2.5° grid

and monthly time step for 16 years. Due to our sample size, our posterior probability dominates over our priors,

4

135 and as with Kelley et al. (2019), priors predominantly were employed to set physically plausible bounds on our parameters.

Once optimized, the model was then run from January 2002 - December 2019 and so the trained model was in a predictive mode for 2019. Due to data availability at the time of writing, July 2017 - June 2018 land cover, land

140 use and population density were recycled for July 2018 onwards (Table S2). We sampled 100 parameter ensemble members from the last 5000 iterations of each of the 10 chains, providing us with 1000 ensemble members to estimate the models' posterior solution to equation 2. The posterior solution, inferred by maximising equation 3, provides an estimate of a burnt area based on the parameter uncertainty of our model, corresponding to the yellow areas in time series in Fig. 1. This was validated as per Kelley et al. (2019), along

145 with additional checks of the models' ability to reproduce seasonality and inter-annual variability of fire. See Fig. S1-S3 and model evaluation supplement for validation methods and results.

In the predictive model, the probability of a burnt area y (where y can be outside training data Y_s, as is the case for our year 2019 analysis), being explained by our model ($P(y)$ - full model uncertainty, or model error, in

150 tan areas on time series in Fig. 1) is proportional to the probability of y given a parameter set, β, weighted by $P(\beta|Y_s)$:

$$P(y) \propto \int_{PS} P(\beta|Y_s) \times P(y|\beta) \, d\beta \qquad (4)$$

where PS is all parameter space.

We chose five regions (marked A-E in Fig. 1 and Fig. S4) to represent forest areas already under pressure from

155 deforestation:

    A. Acre and the Southern Amazonas States in Brazil at the western extent of the "arc of deforestation" in the Tropical Moist Forest

    B. Northern Mato Grosso, Brazil, towards the central regions of the arc of deforestation

    C. Maranhão and Piauí, Brazil, in coastal deforestation regions

160   D. Bolivian dry forest

    E. Paraguay dry forests and woodland

We also assessed an overall Area of Active Deforestation (AAD) in the Amazon region (Fig. S4). This area is defined as the parts of South American southern tropics with significant decreasing tree cover trends, as seen in VCF (Dimiceli et al., 2015) and increasing agricultural fractions in the HYDEv3.1 dataset (Klein Goldewijk et

165 al., 2010). Trend analysis used the same technique described in Kelley et al. (2019).

We assessed the probability of 2019 fire activity being explained by information provided to the model in three ways (Table 1):

1. What was the likelihood of the observed monthly burnt area occurring, which is where the observed
   burnt area falls within the main range e.g. 5%-95% of the model's full posterior (red line vs tan area in
170   the time series in Fig. 1);
2. How likely was it that burnt area would have been higher than the annual average, i.e the fraction of the
   model's full posterior greater than the models annual average climatological posterior (the point where
   the vertical lines cross 1 in right-hand columns in Fig. 1)
3. What was the likelihood of such an anomalous year occurring in the observations? Calculated as the
175   fraction of the models' full posteriors anomaly being greater than the observed anomaly.

3 Results

3.1 Burnt area in 2019 in context

The year 2019 burnt area during the early fire season (defined as June to August) was higher than the 2002-2019
average in areas of recent historic deforestation, despite a lower than average burnt area over much of the rest of
180 the continent (Fig. 2). The AAD as a whole saw the 2nd highest levels of burning in the fire season (Fig. 1F,
August), behind 2010, with 11% of the area experiencing more burning than in any previous year. Burnt area for
what is normally the climatological peak of the fire season in September (Fig. S2-S3) returned to
lower-than-normal levels along the Brazilian arc of deforestation, though remained high along the border
between Brazil, Bolivia and Paraguay (Fig. 1 D, E and 3). This meant that, while the burnt area was higher than
185 usual in 2019, it was not exceptionally higher over the entire fire season (June -September). Other high years
were 2004 in the Bolivian dry forest (red line in Fig. 1D), 2005 in the eastern arc of deforestation (Fig. 1A) and
Paraguay dry forest (Fig. 1E), 2002 in Paraguay, 2007 in monsoonal coastal forests (Fig. 1C) and 2010 in
Bolivia and Paraguay dry forests (Fig. 1C and D). Deforestation rates in 2004/05 were high (Marengo et al.,
2018), whereas 2005 and 2010 burning have previously been associated with droughts driven by a Tropical
190 North Atlantic warming anomaly (Marengo and Espinoza, 2016). The increase in fire activity in 2007 has been
linked to deforestation across the Amazon (Morton et al., 2008).

3.2 Climatic conditions in 2019

The model shows with statistical high confidence that most of Amazonia should have, in fact, experienced less
fire than normal for June-August when accounting for 2019 meteorological conditions. This expected low fire
195 rate included areas in the AAD that saw higher than annual average burning in observations (Fig. 2). Only 2 ±
0% area (i.e. one grid cell throughout the sampled posterior) showed unprecedented high burning in the model.
This is despite a good agreement between the modelled and the observed burnt area in preceding years across all
locations (yellow in time series in Fig. 1), and the model also ranking the order of most previous fire seasons
across the region accurately (Fig. S1-S3 and model evaluation supplement). The model also identifies an
200 increase in burning across the region in the meteorological dry years of 2004/2005 and 2010 (Fig. 1F). The
observed burnt area exceeds the model in all our regions in 2019 (Fig. 1) except region C in the already heavily

converted agricultural land near the Brazilian coast (Fig. S4). While the observed burnt area falls within the full models posterior for regions A-C, for regions D and E it exceeds the 99% confidence interval of the full model posterior for June-September, and in August for the entire deforested region (tan in Fig. 1, Table 1), indicating

205   that the fire levels in 2019 fall outside of the expected range, especially in southern Amazonia.

The observed anomaly for 2019 is higher than the modelled anomaly for August in all regions (Fig. 1, "August" column, red points). This is particularly prominent in regions D and E where the model suggests that meteorological conditions alone should have resulted in a fire season with a 67-89% reduction in burnt area in D and 57-76% for E compared to the August average based on parameter uncertainty, with only a 6% and 8%

210   chance of a greater burnt area than the average for D and E respectively. Observations instead show that burnt area was 45% and 130% greater than the August average (Table 1). Even in regions A and B, where there was a 48% and 22% probability of seeing greater than average burning, the model suggests that the likely burnt area was 42-70% and 71-80% reduction in burnt area compared to the August average. These meteorologically-based estimates are much less than the 154% and 148% increases seen in the observations.

215   There are other anomalous years in individual regions (2014/2015 in region E, which the model suggests should have had a higher burnt area than observed, and 2007, 2012 in C and 2010 in D, where the models suggest less there should have been less fire). However, none are as far outside the model range as 2019. For the AAD, only 2019 is shown to be a significantly anomalous year, with only a 7-8% chance of the levels of burning seen in observations (Table 1), or just 1% in regions B, D and E.

220   **4 Discussion**

The observed spatial pattern of burnt area in June-August 2019 shows that unprecedented burning was only seen in regions normally associated with deforestation. Our modelling framework demonstrates that, based on meteorological conditions alone, reduced burning seen across the rest of Tropical South America should have extended into these regions. Specifically, our analysis suggests that there is only a 7% probability that the levels

225   of burning in the early fire season would have been caused by 2019 meteorological conditions or natural ignitions alone (time series Fig. 1). Eastern areas normally associated with deforestation did show expected levels of burning, but in the western and central parts of the arc of deforestation and Bolivia and Paraguay dry forests, burning was much higher. Here there is a <1% of such anomalous levels of burning compared to the background rate (Fig. 1 "August" column). As we account for deep soil moisture, we can also eliminate the

230   possibility that longer-term drier conditions contributed to the 2019 fires. The cause of increased burning in 2019 is therefore either a driver left static in the model for 2019, or a process not considered. Because of the non-availability of near-real-time data, drivers held unchanged at 2018 values for 2019 are tree cover, land use and human population. The only plausible way tree cover could have substantially changed is through increased deforestation rates (Zhang et al., 2015). Thereby changes in drivers not accounted for in 2019 would only have

235   caused increased burning through direct human manipulation of the landscape rather than the particular meteorological features of that year.

Improved descriptions of evolving changes in human fire and landscape interactions over time may also be required to capture direct human-driven changes in burnt area. This is likely to include changes in demography or human behaviour, for example we currently account for the impact of a changing population on fire starts and

240 suppression, but not how fire ignitions per person change over time. An evolving policy could have also been the cause of the unusual fire activity. It should also be noted that observed fire activity returned to expected levels given meteorological conditions in September in the Northern end of the deforestation region (Fig. 1, 3). This reduction could be after the June-August fires received international media coverage, triggering efforts in combating fires from South American governments (BBC news, 2019; NASA, 2019).

245 **5 Conclusion**

In this study, we have used a novel Bayesian modelling approach to track uncertainties in modelling fire in the land surface. Our framework provides a rapid assessment of whether there was any influence of meteorological conditions across the Amazon that exacerbated fire levels in 2019.

The model predicts a lower burnt area than we see in the observations for Amazonia during June-August 2019,
250 indicating that from observed meteorological data alone, we would not expect 2019 to be a high-fire year. This result points strongly to the importance of including socio-economic factors having a strong role in the high recorded fire activity. Specifically, we conclude that it is likely (93% probability) based on past relationships between burnt area and meteorological conditions, that the weather conditions did not trigger the increase in burning in Amazonia during the early fire season in 2019. This result holds over the entire area of active
255 deforestation and furthermore is extremely likely (>99%) in central and Southeastern Amazonia.

Code/Data Availability

265 The model code and Bayesian inference framework used to support the findings of this study are archived at https://doi.org/10.5281/zenodo.3817456. Model output is archived at https://doi.org/10.5281/zenodo.3817467. Driving data availability is listed in Table S1.

Author contributions

270 DK, CB, MB and CH developed the modelling framework; RW designed the Bayesian inference framework; DK, MB and ND collated and regridded input data. DK, CB, CH performed the analysis. CB wrote the first draft of the paper with input from DK, CH and ND. All authors contributed to the final manuscript. The authors declare no competing interests.

References

275 Adler, R. F., Huffman, G. J., Chang, A., Ferraro, R., Xie, P.-P., Janowiak, J., Rudolf, B., Schneider, U., Curtis, S., Bolvin, D., Gruber, A., Susskind, J., Arkin, P. and Nelkin, E.: The Version-2 Global Precipitation Climatology Project (GPCP) Monthly Precipitation Analysis (1979–Present), J. Hydrometeorol., 4(6), 1147–1167, 2003.

Aldersley, A., Murray, S. J. and Cornell, S. E.: Global and regional analysis of climate and human 280 drivers of wildfire, Sci. Total Environ., 409(18), 3472–3481, 2011.

Andela, N., Morton, D. C., Giglio, L., Chen, Y., van der Werf, G. R., Kasibhatla, P. S., DeFries, R. S., Collatz, G. J., Hantson, S., Kloster, S., Bachelet, D., Forrest, M., Lasslop, G., Li, F., Mangeon, S., Melton, J. R., Yue, C. and Randerson, J. T.: A human-driven decline in global burned area, Science, 356(6345), 1356–1362, 2017.

285 Andrade, R. de O.: Alarming surge in Amazon fires prompts global outcry, Nature, 2019.

Aragão, L. E. O. C., Anderson, L. O., Fonseca, M. G., Rosan, T. M., Vedovato, L. B., Wagner, F. H., Silva, C. V. J., Silva Junior, C. H. L., Arai, E., Aguiar, A. P., Barlow, J., Berenguer, E., Deeter, M. N., Domingues, L. G., Gatti, L., Gloor, M., Malhi, Y., Marengo, J. A., Miller, J. B., Phillips, O. L. and Saatchi, S.: 21st Century drought-related fires counteract the decline of Amazon deforestation carbon 290 emissions, Nat. Commun., 9(1), 536, 2018.

Arruda, D., Candido, H. G. and Fonseca, R.: Amazon fires threaten Brazil's agribusiness, Science, 365(6460), 1387, 2019.

BBC news: Amazon fires: Brazil bans land clearance blazes for 60 days, BBC news [online] Available from: https://www.bbc.co.uk/news/world-latin-america-49507405 (Accessed 3 November 295 2020), 2019.

Bivand, R., Keitt, T. and Rowlingson, B.: rgdal: Bindings for the Geospatial Data Abstraction Library, [online] Available from: http://CRAN.R-project.org/package=rgdal, 2016.

Boer, M. M., de Dios, V. R. and Bradstock, R. A.: Unprecedented burn area of Australian mega forest fires, Nat. Clim. Chang., 10(3), 171–172, 2020.

300 Brando, P. M., Balch, J. K. and Nepstad, D. C.: Abrupt increases in Amazonian tree mortality due to drought–fire interactions, Proceedings of the [online] Available from: https://www.pnas.org/content/111/17/6347.short, 2014.

Burton, C., Betts, R. A. and Jones, C. D.: Will fire danger be reduced by using Solar Radiation Management to limit global warming to 1.5 C compared to 2.0 C?, Geophys. Res. Lett. [online] 305 Available from: https://agupubs.onlinelibrary.wiley.com/doi/abs/10.1002/2018GL077848, 2018.

Butler, R.: Calculating deforestation figures for the Amazon, Rio de Janeiro, 2017.

Cochrane, M. A. and Schulze, M. D.: Fire as a Recurrent Event in Tropical Forests of the Eastern Amazon: Effects on Forest Structure, Biomass, and Species Composition1, Biotropica, 31(1), 2–16, 1999.

310 De Groot, W. J., Goldammer, J. G., Justice, C. O. and Lynham, T. J.: Implementing a global early warning system for wildland fire, Proc. Virchow. Pirquet. Med. Soc., 2010.

Dimiceli, C., Carroll, M., Sohlberg, R., Kim, D. H., Kelly, M. and Townshend, J. R. G.: MOD44B MODIS/Terra Vegetation Continuous Fields Yearly L3 Global 250m SIN Grid V006, , doi:10.5067/MODIS/MOD44B.006, 2015.

315 Escobar, H.: Amazon fires clearly linked to deforestation, scientists say, Science, 365(6456), 853, 2019.

Fisher, R. A. and Koven, C. D.: Perspectives on the future of Land Surface Models and the challenges of representing complex terrestrial systems, J. Adv. Model. Earth Syst., doi:10.1029/2018MS001453, 2020.

320 Fonseca, M. G., Alves, L. M., Aguiar, A. P. D., Arai, E., Anderson, L. O., Rosan, T. M., Shimabukuro, Y. E. and Aragão, L. E. O. e. C.: Effects of climate and land-use change scenarios on fire probability during the 21st century in the Brazilian Amazon, Glob. Chang. Biol., 25(9), 2931–2946, 2019.

GDAL/OGR contributors: GDAL/OGR Geospatial Data Abstraction software Library, Open Source Geospatial Foundation. [online] Available from: http://gdal.org, 2018.

325 Giglio, L., Boschetti, L., Roy, D. P., Humber, M. L. and Justice, C. O.: The Collection 6 MODIS burned area mapping algorithm and product, Remote Sens. Environ., 217, 72–85, 2018.

de Groot, W. J., Wotton, B. M. and Flannigan, M. D.: Chapter 11 - Wildland Fire Danger Rating and Early Warning Systems, in Wildfire Hazards, Risks and Disasters, edited by J. F. Shroder and D. Paton, pp. 207–228, Elsevier, Oxford., 2015.

330 Hantson, S., Arneth, A., Harrison, S. P., Kelley, D. I., Prentice, I. C., Rabin, S. S., Archibald, S., Mouillot, F., Arnold, S. R., Artaxo, P., Bachelet, D., Ciais, P., Forrest, M., Friedlingstein, P., Hickler, T., Kaplan, J. O., Kloster, S., Knorr, W., Laslop, G., Li, F., Melton, J. R., Meyn, A., Sitch, S., Spessa, A., van der Werf, G. R., Voulgarakis, A. and Yue, C.: The status and challenge of global fire modelling, Biogeosciences, 13(11), 3359–3375, 2016.

335 Hantson, S., Kelley, D. I., Arneth, A., Harrison, S. P., Archibald, S., Bachelet, D., Forrest, M., Hickler, T., Lasslop, G., Li, F., Mangeon, S., Melton, J. R., Nieradzik, L., Rabin, S. S., Colin Prentice, I., Sheehan, T., Sitch, S., Teckentrup, L., Voulgarakis, A. and Yue, C.: Quantitative assessment of fire and vegetation properties in historical simulations with fire-enabled vegetation models from the Fire Model Intercomparison Project, Geoscientific Model Development Discussions,
340 doi:10.5194/gmd-2019-261, 2020.

Hijmans, R. J. and van Etten, J.: raster: Geographic data analysis and modeling, R package version, 2(8), 2014.

INPE: INPE Fire Count Data, [online] Available from: http://queimadas.dgi.inpe.br/queimadas/portal-static/estatisticas_paises/ (Accessed 2019), 2019.

345 Jolly, W. M., Cochrane, M. A., Freeborn, P. H., Holden, Z. A., Brown, T. J., Williamson, G. J. and

Bowman, D. M. J. S.: Climate-induced variations in global wildfire danger from 1979 to 2013, Nat. Commun., 6, 7537, 2015.

Jones, M. W., Smith, A., Betts, R., Canadell, J. G. ., Prentice, I. C. and Le Quéré, C.: Climate change increases the risk of wildfires, ScienceBrief Review, 2020.

350   Kalnay, E., Kanamitsu, M., Kistler, R., Collins, W., Deaven, D., Gandin, L., Iredell, M., Saha, S., White, G., Woollen, J., Zhu, Y., Chelliah, M., Ebisuzaki, W., Higgins, W., Janowiak, J., Mo, K. C., Ropelewski, C., Wang, J., Leetmaa, A., Reynolds, R., Jenne, R. and Joseph, D.: The NCEP/NCAR 40-Year Reanalysis Project, Bull. Am. Meteorol. Soc., 77(3), 437–472, 1996.

Kelley, D. I.: Modelling Australian fire regimes, Ph.D., Macquarie University., 2014.

355   Kelley, D. I. and Harrison, S. P.: Enhanced Australian carbon sink despite increased wildfire during the 21st century, Environ. Res. Lett., 9(10), 104015, 2014.

Kelley, D. I., Harrison, S. P. and Prentice, I. C.: Improved simulation of fire–vegetation interactions in the Land surface Processes and eXchanges dynamic global vegetation model (LPX-Mv1), Geoscientific Model Development, 7(5), 2411–2433, 2014.

360   Kelley, D. I., Bistinas, I., Whitley, R., Burton, C., Marthews, T. R. and Dong, N.: How contemporary bioclimatic and human controls change global fire regimes, Nat. Clim. Chang., 9(9), 690–696, 2019.

Klein Goldewijk, K., Goldewijk, K. K., Beusen, A., Van Drecht, G. and De Vos, M.: The HYDE 3.1 spatially explicit database of human-induced global land-use change over the past 12,000 years, Glob. Ecol. Biogeogr., 20(1), 73–86, 2010.

365   Krawchuk, M. A. and Moritz, M. A.: Burning issues: statistical analyses of global fire data to inform assessments of environmental change, Environmetrics, 25(6), 472–481, 2014.

Lasslop, G., Brovkin, V., Reick, C. H., Bathiany, S. and Kloster, S.: Multiple stable states of tree cover in a global land surface model due to a fire-vegetation feedback, Geophys. Res. Lett., 43(12), 6324–6331, 2016.

370   Lizundia-Loiola, J., Pettinari, M. L. and Chuvieco, E.: Temporal Anomalies in Burned Area Trends: Satellite Estimations of the Amazonian 2019 Fire Crisis, Remote Sensing, 12(1), 151, 2020.

Lovejoy, T. E. and Nobre, C.: Amazon tipping point: Last chance for action, Sci Adv, 5(12), eaba2949, 2019.

Marengo, J. A. and Espinoza, J. C.: Extreme seasonal droughts and floods in Amazonia: causes, 375   trends and impacts: EXTREMES IN AMAZONIA, Int. J. Climatol., 36(3), 1033–1050, 2016.

Marengo, J. A., Souza, C. A., Thonicke, K., Burton, C., Halladay, K., Betts, R. A., Soares, W. R. and Others: Changes in climate and land use over the Amazon Region: current and future variability and trends, Front Earth Sci. Chin., 6, 228, 2018.

Met Office: Iris: A Python library for analysing and visualising meteorological and oceanographic 380   data sets, v1.2 ed., Exeter, Devon. [online] Available from: http://scitools.org.uk/, 2013.

Morton, D. C., Defries, R. S., Randerson, J. T., Giglio, L., Schroeder, W. and Van Der Werf, G. R.: Agricultural intensification increases deforestation fire activity in Amazonia, Glob. Chang. Biol., 14(10), 2262–2275, 2008.

NASA: Uptick in Amazon Fire Activity in 2019, NASA Earth Observatory [online] Available from:

385   https://www.earthobservatory.nasa.gov/images/145498/uptick-in-amazon-fire-activity-in-2019
        (Accessed 3 November 2020), 2019.

        Nauslar, N. J., Brown, T. J., McEvoy, D. J. and Lareau, N. P.: Record-setting 2018 California
        wildfires, in State of the Climate 2018, edited by J. A. D. S. A. Blunden, p. 195, Bulletin of the
        American Meteorological Society., 2019.

390   van Oldenborgh, G. J., Krikken, F., Lewis, S., Leach, N. J., Lehner, F., Saunders, K. R., van Weele,
        M., Haustein, K., Li, S., Wallom, D., Sparrow, S., Arrighi, J., Singh, R. P., van Aalst, M. K., Philip, S.
        Y., Vautard, R. and Otto, F. E. L.: Attribution of the Australian bushfire risk to anthropogenic climate
        change, Natural Hazards and Earth System Sciences Discussions, doi:10.5194/nhess-2020-69, 2020.

        Patel, K.: Arctic Fires Fill the Skies with Soot, NASA Earth Observatory [online] Available from:
395   https://earthobservatory.nasa.gov/images/145380/arctic-fires-fill-the-skies-with-soot (Accessed 1
        December 2019), 2019.

        Pellegrini, A. F. A., Anderegg, W. R. L., Paine, C. E. T., Hoffmann, W. A., Kartzinel, T., Rabin, S. S.,
        Sheil, D., Franco, A. C. and Pacala, S. W.: Convergence of bark investment according to fire and
        climate structures ecosystem vulnerability to future change, Ecol. Lett., 20(3), 307–316, 2017.

400   Perry, J. J., Cook, G. D., Graham, E., Meyer, C. P. M., Murphy, H. T. and VanDerWal, J.: Regional
        seasonality of fire size and fire weather conditions across Australia's northern savanna, Int. J.
        Wildland Fire, 29(1), 1–10, 2020.

        Prentice, I. C., Harrison, S. P. and Bartlein, P. J.: Global vegetation and terrestrial carbon cycle
        changes after the last ice age, New Phytol., 189(4), 988–998, 2011a.

405   Prentice, I. C., Kelley, D. I., Foster, P. N., Friedlingstein, P., Harrison, S. P. and Bartlein, P. J.:
        Modeling fire and the terrestrial carbon balance, Global Biogeochem. Cycles, 25(3),
        doi:10.1029/2010gb003906, 2011b.

        Rabin, S. S., Melton, J. R., Lasslop, G., Bachelet, D., Forrest, M., Hantson, S., Li, F., Mangeon, S.,
        Yue, C., Arora, V. K. and Others: The Fire Modeling Intercomparison Project (FireMIP), phase 1:
410   Experimental and analytical protocols, Geoscientific Model Development, 20, 1175–1197, 2017.

        R Core Team: R: A Language and Environment for Statistical Computing, [online] Available from:
        http://www.R-project.org/, 2015.

        RFS: New South Wales Rural Fire Service, [online] Available from:
        https://www.rfs.nsw.gov.au/fire-information/fires-near-me (Accessed 2019), 2019.

415   Salvatier, J., Wiecki, T. V. and Fonnesbeck, C.: Probabilistic programming in Python using PyMC3,
        PeerJ Comput. Sci., 2, e55, 2016.

        Sanderson, B. M. and Fisher, R. A.: A fiery wake-up call for climate science, Nat. Clim. Chang.,
        10(3), 175–177, 2020.

        Tollefson, J.: ECOLOGY Huge wildfires defy explanation, Nature, 561(7721), 16–17, 2018.

420   Van Der Werf, G. R., Randerson, J. T., Giglio, L., Gobron, N. and Dolman, A. J.: Climate controls on
        the variability of fires in the tropics and subtropics, Global Biogeochem. Cycles, 22(3) [online]
        Available from: https://agupubs.onlinelibrary.wiley.com/doi/abs/10.1029/2007GB003122, 2008.

        Williams, A. P. and Abatzoglou, J. T.: Recent Advances and Remaining Uncertainties in Resolving
        Past and Future Climate Effects on Global Fire Activity, Current Climate Change Reports, 2(1), 1–14,

425 2016.

Wiltshire, J., Hekman, J. and Milan, B. F.: Carbon loss and economic impacts of a peatland wildfire in north-east Sutherland, Scotland, 12-17 May 2019, WWF-UK., 2019.

Zeppel, M. J. B., Harrison, S. P., Adams, H. D., Kelley, D. I., Li, G., Tissue, D. T., Dawson, T. E., Fensham, R., Medlyn, B. E., Palmer, A., West, A. G. and McDowell, N. G.: Drought and resprouting
430 plants, New Phytol., 206(2), 583–589, 2015.

Zhang, K., de Almeida Castanho, A. D., Galbraith, D. R., Moghim, S., Levine, N. M., Bras, R. L., Coe, M. T., Costa, M. H., Malhi, Y., Longo, M., Knox, R. G., McKnight, S., Wang, J. and Moorcroft, P. R.: The fate of Amazonian ecosystems over the coming century arising from changes in climate, atmospheric CO2,and land use, Global Change Biology, 21(7), 2569–2587, doi:10.1111/gcb.12903,
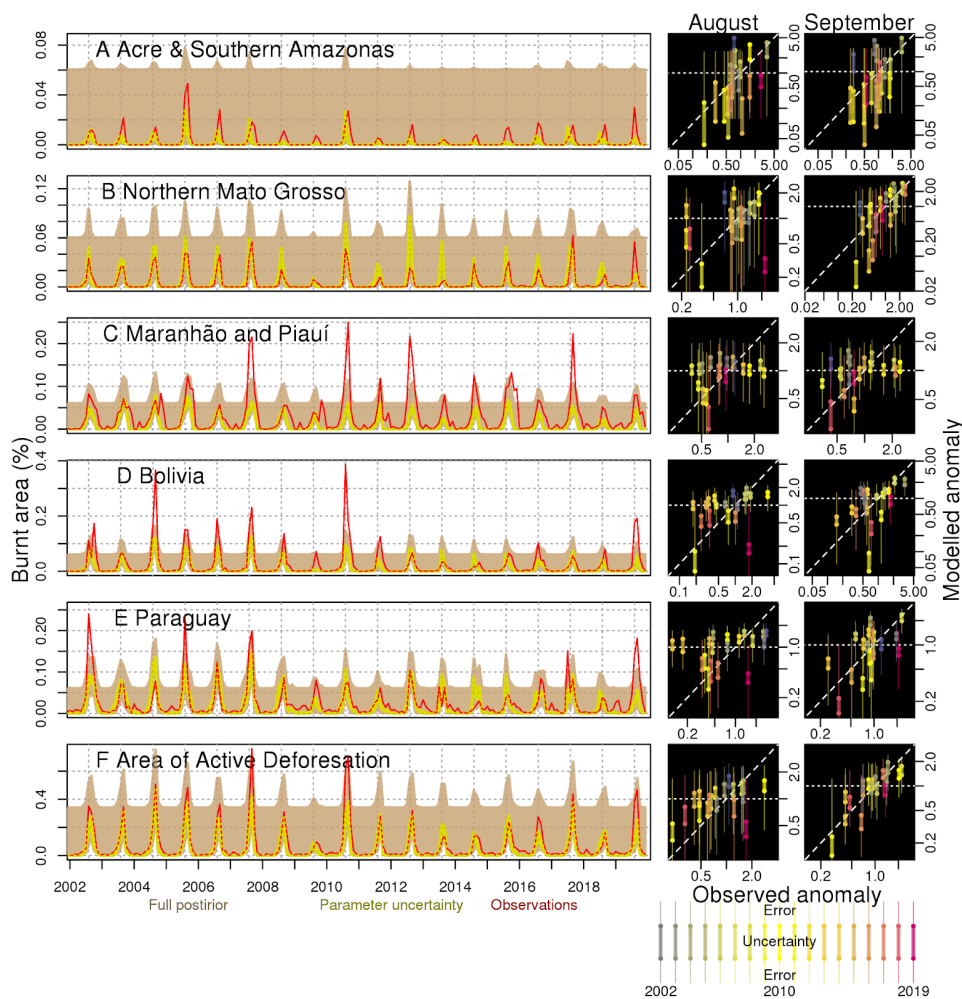435 2015.

Figure 1: Time series and fire season anomalies for modelled and observed burnt area. Top 5 rows show regions A - E, while the bottom row shows F, the "Area of Active Deforestation" region which incorporates areas where there has been a significant increase in agriculture and decrease in tree cover. See Fig. S4 for location. Red lines show monthly burnt area observations from MCD64A1, yellow shows model accounting for parameter uncertainty (5-95%) and brown shows full model uncertainty (5-95%). The red line is dashed when observations and model accounting for parameter uncertainty overlap. Vertical grid lines are positioned for August each year. Right-hand plots show observed (x-axis) and modelled (y-axis) anomaly, calculated as 2019 burnt area over 2002-2019 climatological average burnt area for (first column) August and (second column) September. Thin lines show 5-95% full model uncertainty, while dots and thick line indicate 5% and 95% parameter uncertainty.
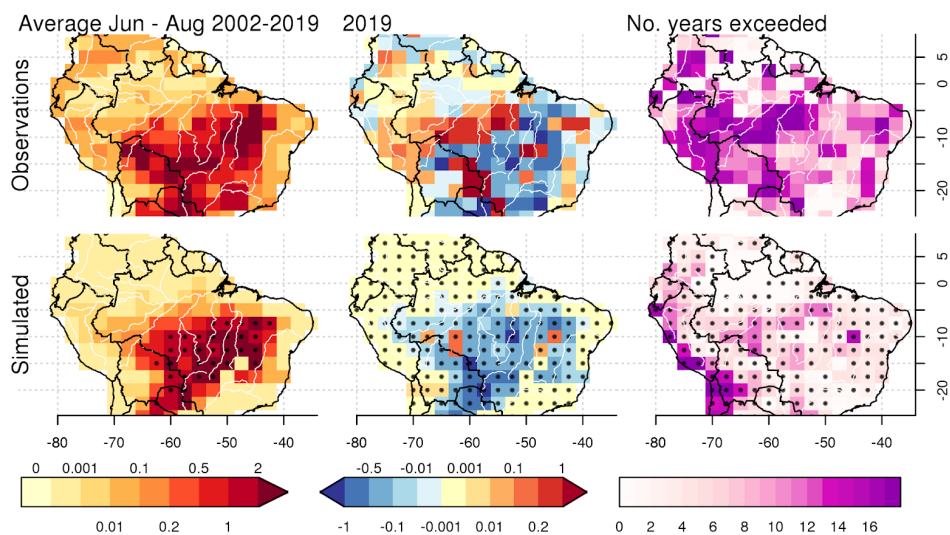
Figure 2: Maps of modelled and observed % burnt area. First row: observed burnt area, June-August 2002-2019 annual average (left) and anomaly in 2019 (centre), and the number of years 2019 burnt area exceeds (right). Second row: as top row, as simulated by the model. Annual stippling represents where the 5% percentile > half the 95% percentile of models posterior, 2019 anomaly stripling when 95% of the models posterior agree on the direction of the anomaly, and no of years stippling when 95% of the models posterior agree on the number of years 2019 exceeds.
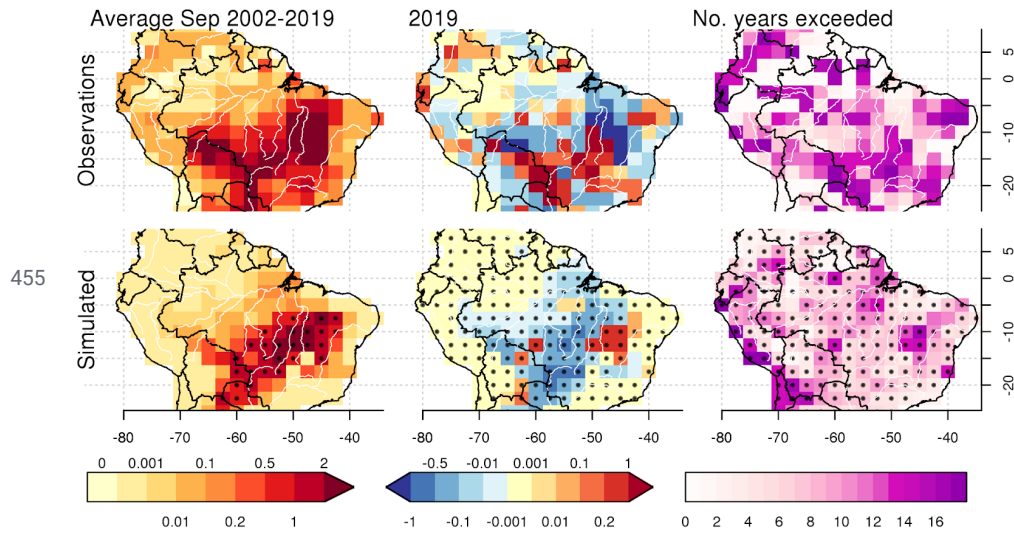
450

15

Figure 3: Same as Fig. 2 but for September.

Biogeosciences
Discussions

Open Access

EGU

Table 1: Observed and model anomaly in burnt area for August and September 2019 as a fraction of August and September averages 2002-2019 across selected regions (see methods). Red indicates more burning than normal, blue less and yellow around average burning. The model is expressed as 5-95% of the posterior accounting for parameter

460 **uncertainty. Likelihood gives the percentage probability that (1st column) the observed burnt area is suggested by the model (2nd) that the model suggests a higher than average burnt area for the given month, and (3rd) that the model captures the observed anomaly based on the full model posterior.**

Regions		Observed anomaly	Model anomaly		Likelihood (%)		
			5%	95%	Burnt area	Higher than average	Anomaly
A	Aug 2019	2.539	0.296	0.584	37	48	8
	Sep 2019	0.758	0.149	0.689	75	49	59
B	Aug 2019	2.484	0.200	0.292	13	22	1
	Sep 2019	1.008	0.49	1.089	61	43	43
C	Aug 2019	0.812	0.245	0.413	12	45	60
	Sep 2019	0.607	0.225	0.592	22	41	80
D	Aug 2019	1.454	0.106	0.330	1	6	1
	Sep 2019	1.650	0.472	0.812	1	45	7
E	Aug 2019	2.303	0.239	0.428	1	8	1
	Sep 2019	2.664	0.519	0.707	1	35	1
F	Aug 2019	1.596	0.280	0.630	8	29	7
	Sep 2019	1.248	0.402	1.187	13	45	26

465